ARCENG
INTERNATIONAL JOURNAL OF ARCHITECTURE AND ENGINEERING
ISSN
2822-6895

Article Arrival Date
12.11.2025

Article Published Date
20.12.2025

Effects of First Story Stiffness on Earthquake Responses of 2-Story Wooden Houses

Koichi KIMURA

Dr., Japan Ground Self Defense Force, Tohoku Depot, Supply Department, Orcid:0000-0002-2050-7429

Abstract

In this study, a seismic response analysis of 2-story wooden houses has been carried out, and guidelines for proper seismic rehabilitation have been considered. In the analysis, the bilinear + slip model is adopted as the restoring-force characteristics because in previous studies it has been confirmed that the model reproduces characteristics of wooden houses relatively well. First, it was investigated how much the first story stiffness affects the inertia force of the roof during an earthquake. Next, the effects of roof mass were examined. Finally, in the case where an anti-seismic shelter was placed on the ground floor, a suitable connection method to the house was considered.

Keywords: Restoring-Force Characteristics, Bilinear + Slip Model, Wooden House, Earthquake Resistance, Seismic Response Time History Analysis, Anti-Seismic Shelter, Oil Damper, Pushover Analysis

1. INTRODUCTION

For an earthquake countermeasure, we performed construction work in which a steel shelter (manufactured by Tobu Bousai Construction in Japan) was installed in the first story of a 2-story wooden frame house in Toride City (Fig. 1), which was located about 350km south-west of the epicentre of the 2011 off the Pacific Coast of Tohoku Earthquake, from August to September 2013. Although the installation of an earthquake-resistant shelter is usually intended to secure safe space in a part of the building and not to reinforce the entire structure, in this case the shelter was tightly connected to the ceiling beams of the first story to increase the story stiffness. This method has been often adopted as a seismic countermeasure for existing houses because it can be done while residents are still living in the house, and it is more advantageous than seismic isolation in terms of cost and construction period. However, on September 20, 2013, the day immediately after the construction work, by getting caught in a relatively small earthquake which could be considered as one of aftershocks of the 2011 off the Pacific Coast of Tohoku Earthquake, the tile roof underwent partial breakdown. Although the main shock on March 11, 2011 was followed by many large aftershocks, there had been no damage to this house until that aftershock. Since this incident occurred immediately after seismic reinforcement work was done, I hypothesized that this work increased the stiffness of the first story, which increased the inertia force of the roof. Hence, firstly, the effects of first story stiffness on the inertia force of the roof during an earthquake are investigated by numerical simulations. After that, the effects of roof mass and a suitable connection method between the house and the anti-seismic shelter are considered with the goal of establishing guidelines for

more effective seismic reinforcement.

There have been several previous studies related to this study. Araki et al. [1] proposed a method to predict the hysteresis model of a whole wooden house by summation of the parameters of hysteresis models for resisting shear walls. Nakayama and Kojima [2] approximately evaluated the elastic-plastic response of a 2-story wooden house subjected to the critical pulse-like ground motion by using the reduction method into the single-degree-of-freedom system and the closed-form solution derived by themselves. Matsumoto et al. [3] investigated the response reduction effect for existing wooden houses to which a seismic shelter was connected with oil dampers by time history (seismic) response analysis [4, 5] using the collapsing simulation program wallstat [6, 7]. In order to make it easier to compare with those previous studies, M-1 in the paper of Araki et al. [1] and the NS component of Kobe Earthquake (1995) acceleration record are used as the base model for time history response analysis and the input seismic wave, respectively. Although M-1 is different from the above-mentioned house in Toride City, this model can be regarded as a typical Japanese 2-story wooden house. The bilinear + slip model [1, 2], which reproduces characteristics of wooden houses relatively well, is adopted as the restoring-force characteristics of target models.

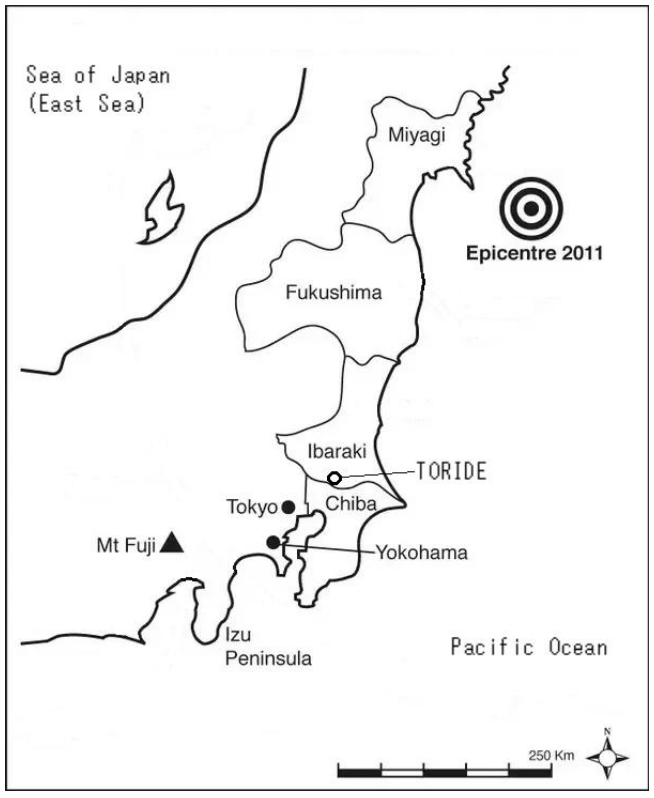

Figure 1. Locations of Toride City in Ibaraki Prefecture, Japan, and the epicentre of the 2011 off the Pacific Coast of Tohoku Earthquake.

2. EQUATIONS OF MOTION FOR 2-STORY STRUCTURES SUBJECTED TO GROUND MOTION

2.1. Linear Motion Equations for the 2-Mass System

First, the vibration equations for the 2-mass system subjected to ground motion u (Fig. 2) are derived in the following. It is assumed that the damping force of each story is proportional to

ISSN
2822-6895

its relative velocity. In accordance with D'Alembert's principle the equilibrium equations of mass points 1 and 2 may be written as

$$k_2(x_2 - x_1) + C_2(\dot{x}_2 - \dot{x}_1) - k_1 x_1 - C_1 \dot{x}_1 + [-m_1(\ddot{u} + \ddot{x}_1)] = 0 \quad (1)$$

and

$$-k_2(x_2 - x_1) - C_2(\dot{x}_2 - \dot{x}_1) + [-m_2(\ddot{u} + \ddot{x}_2)] = 0 \quad (2)$$

respectively. Here, u is the horizontal displacement of the ground, x_1 and x_2 are the displacements relative to the ground, m_1 is the point mass 1 (weight of story 1's upper half + story 2's lower half), m_2 is the point mass 2 (weight of story 2's upper half + roof truss), k_1 and k_2 are the horizontal stiffnesses, and C_1 and C_2 are the damping coefficients. Reorganizing Eqs. (1) and (2), we obtain the following equations:

$$m_1(\ddot{u} + \ddot{x}_1) + f_{D1} - f_{D2} + f_{R1} - f_{R2} = 0 \quad (3)$$

$$m_2(\ddot{u} + \ddot{x}_2) + f_{D2} + f_{R2} = 0 \quad (4)$$

where

$$f_{D1} = C_1 \dot{x}_1, \quad f_{D2} = C_2(\dot{x}_2 - \dot{x}_1) \quad (5)$$

are the damping forces,

$$f_{R1} = k_1 x_1, \quad f_{R2} = k_2(x_2 - x_1) \quad (6)$$

are the restoring forces.

Eqs. (5) and (6) may be applied only in cases where a structure responds in the linear range. However, it can be predicted that the response of a structure far exceeds the linear range during a large earthquake. Thus the cases in which a structure responds in the nonlinear range beyond the linear range are described in the following.

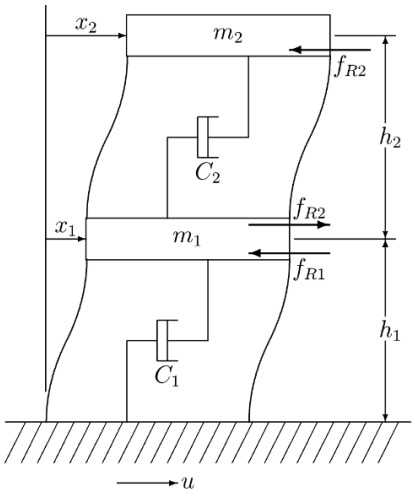

Figure 2. Two-mass model.

2.2. Viscous Damping Characteristics in the Plastic Region

When the response of a vibration system enters the plastic zone, hysteretic damping (energy consumption by hysteresis characteristics) appears in addition to viscous damping. In the process of sequentially analyzing the equations of motion, the hysteretic damping

ISSN
2822-6895

characteristics are evaluated not in terms of damping forces but in terms of the restoring forces (load-deformation relationships), and the viscous damping characteristics are still represented by the terms related to damping forces even in the plastic region. The evaluation of viscous damping characteristics, even in the linear region, is more imprecise and difficult than that of mass and stiffness, and reassessing it in the plastic region is even more difficult. In the analysis, the viscous damping is often assumed to be proportional to the stiffness, but in the nonlinear region, the viscous damping may be set to be proportional to the instantaneous stiffness instead of the initial stiffness, since the apparent stiffness changes with time. This is called instantaneous stiffness-proportional damping, and its viscous damping coefficients are smaller than those of instantaneous stiffness-proportional damping. In response analysis, the damping matrices for initial stiffness and instantaneous stiffness proportionalities are generally obtained by

$$\boldsymbol{C} = \alpha \boldsymbol{K}_e, \quad \alpha = 2h/\omega_e \tag{7}$$

and

$$\boldsymbol{C} = \alpha_p \boldsymbol{K}_p, \quad \alpha_p = \alpha \quad \text{in the usual case} \tag{8}$$

respectively. Here,

$$\boldsymbol{C} = \begin{bmatrix} C_1 + C_2 & -C_2 \\ -C_2 & C_2 \end{bmatrix}$$

is the damping matrix, h is the viscous damping factor, ω_e is the elastic 1st mode circular frequency, $\boldsymbol{K}_e$ is the initial stiffness matrix, and $\boldsymbol{K}_p$ is the instantaneous stiffness matrix. In the plastic region, the hysteretic damping tends to be larger than the viscous damping. As for the evaluation of viscous damping characteristics in this region, there is no significant difference between initial stiffness and instantaneous stiffness proportionalities under a general condition. Hence, in this paper, the damping is treated simply as an initial stiffness proportionality.

2.3. Restoring-Force Characteristics (Bilinear + Slip Model)

The restoring forces $f_{Rj}(t)$ (j = floor number = 1, 2) vary greatly depending on the type of structure (e.g., reinforced concrete, steel-frame, wood construction). The difference in restoring forces, which depends on this structure type, is handled by what is called the restoring force model or the hysteresis model. The features of the restoring-force characteristics of a typical wooden house include the slip phenomenon caused by wood embedments at joints, joint reinforcement hardwares, and the pinching phenomenon, in which the hysteresis area becomes small when shear slip is predominant. The slip-type restoring-force characteristics are used to reproduce the slip phenomenon due to wood embedments, and the bilinear-type restoring-force characteristics are used to reproduce the properties of steel. In addition, the pinching phenomenon is reproduced by using a composite type that is a combination of the bilinear type and the slip type. Hence, in this study, the composite type (bilinear yielding precedence type) is used to model the restoring-force characteristics in order to simultaneously reproduce the three phenomena and functions of wooden houses. The schematic diagram of the restoring-force characteristics and its parameters are shown in Fig. 3 and Table 1, respectively. The relationship between the horizontal stiffnesses k_j and the rotational stiffnesses $(K_i)_j$ is expressed by the following equation:

$$k_{ij} = (K_i)_j / h_j \quad \text{at} \quad i = 1, 2 \text{ or } 3, \quad j = 1, 2 \tag{9}$$

where h_j are the story heights.

ISSN
2822-6895

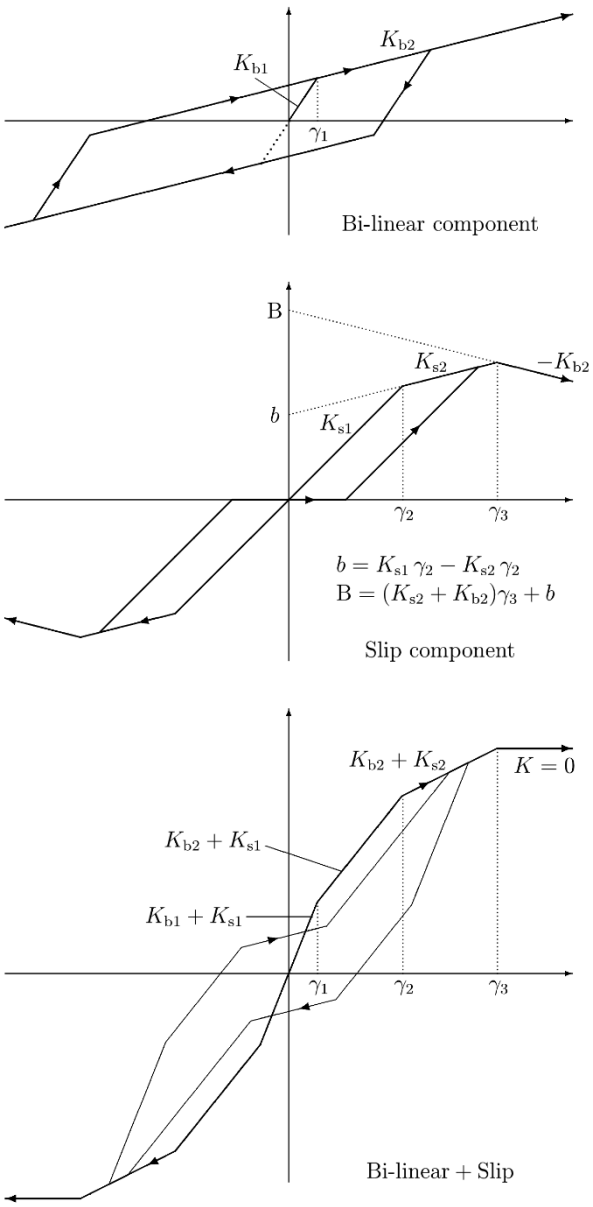

Figure 3. Bilinear and slip-type restoring-force characteristics, and notation of parameters (reprinted from Fig. 2 in Ref. 1).

Table 1. Parameters of the restoring-force model

1st yielding point γ_1 [rad]	0.0020
2nd yielding point γ_2 [rad]	0.0052
3rd yielding point γ_3 [rad]	0.0300
Initial stiffness $(K_1)_j = (K_{b1})_j + (K_{s1})_j$ [N/rad]	$S_j \times 20.140 \times 10^6$

ISSN
2822-6895

2nd stiffness $(K_2)_j = (K_{b2})_j + (K_{s1})_j$ [N/rad]	$S_j \times 15.440 \times 10^6$
3rd stiffness $(K_3)_j = (K_{b2})_j + (K_{s2})_j$ [N/rad]	$S_j \times 3.5000 \times 10^6$
Initial stiffness of the bilinear component $(K_{b1})_j$ [N/rad]	$S_j \times 5.4378 \times 10^6$

Table 2. Mass and height of each story

	Mass [kg]		Height of story [m]
1st story	m_1	9300	h_1	2.885
2nd story	m_2	$R \times 9000$	h_2	2.930

3. ANALYSIS

The target model is the 2-mass shear system as shown in Fig. 2, and the stiffness and weight of each story are shown in Tables 1 and 2, respectively. The damping model was assumed to be of the initial stiffness proportional type with a damping factor of $h = 0.05$. The NS component of Kobe Marine Observatory waves (Maximum $\text{acceleration} = 818$gal) of the Great Hanshin Earthquake (1995) was used as the input ground acceleration. As a numerical method for solving simultaneous ordinary differential equations (3) and (4) with four unknowns, the constant acceleration procedure [8], which is easy to program, was adopted with a time step size of 0.001seconds. Fig. 4 shows the seismic acceleration wave and the response displacement of the base model. From the comparison with the results of the full-scale experiments in the paper of Araki et al. [1], it can be judged that the accuracy of the computer program the author wrote for the analysis is assured.

3.1. Effect of First Story Stiffness on the Inertia Force of Roof

The effect of changing the first story stiffness of the base model on the maximum absolute value $|m_2(\ddot{u} + \ddot{x}_2)|_{\max}$ of the inertia force of mass point 2 (roof section) is shown in Fig. 5. In general, as the stiffness increases, the inertia force decreases and gradually approaches that value obtained when the first story stiffness is rigid (equivalent to a one-mass system). However, since the maximum inertia force increases up to $S_1 = 1.8$ in the graph of Fig. 5, it can be said that the inertia force of the roof section may become excessive due to the increase of first story stiffness. Hence, if an anti-seismic shelter is installed, not only the shelter should be connected to the ceiling beams of the first story, but also the stiffness of the second story should be increased or the roof should be lightened in order to improve the earthquake resistance more effectively.

3.2. Effect of Weight of Roof on the Time History Response

Next, the effect of weight of the roof is considered. Fig. 6 shows the relationship between the mass m_2 of the roof section versus the maximum absolute value $|x_1|_{\max}$ of the displacement of mass point 1 and the maximum absolute value $|m_2(\ddot{u} + \ddot{x}_2)|_{\max}$ of the inertia force of mass point 2 (roof section). It is easy to predict that a lighter roof section reduces the inertia force, and from this graph, it can be seen that not only that, but also the reduction in response

displacement is remarkable, and therefore, the lightening of the roof is effective in improving the earthquake resistance.

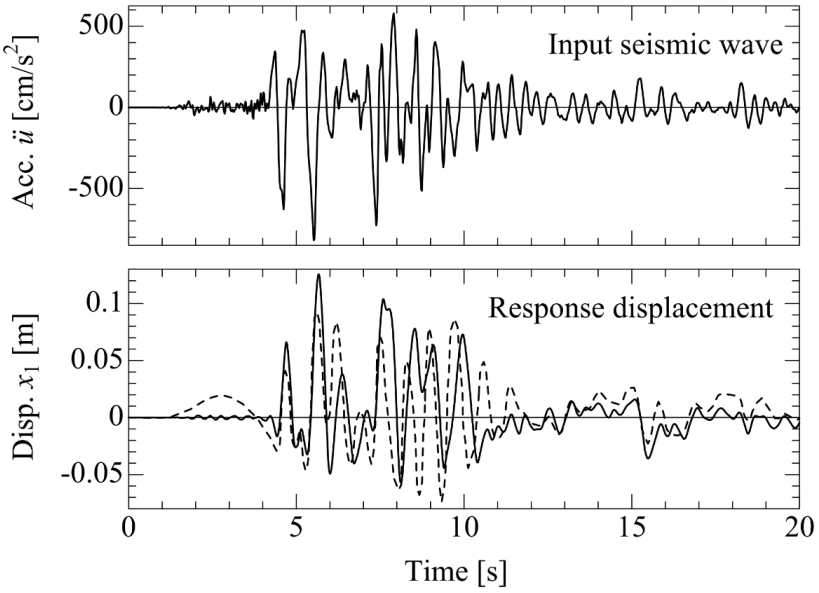

Figure 4. Seismic acceleration wave observed at Kobe Marine Observatory (NS component, Maximum $\mathbf{acceleration = 818}$gal) and response displacement $\boldsymbol{x_1}$ of the base model: dashed curve, Exp. (Ref. 1).

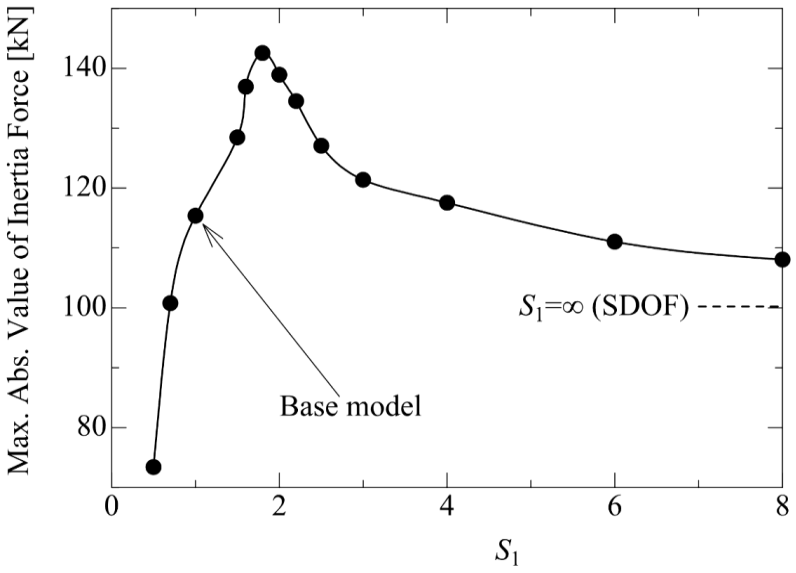

Figure 5. Relation between stiffness of the first story and maximum absolute value of inertia force of $\boldsymbol{m_2}$ ($\boldsymbol{S_2 = 1}$, $\boldsymbol{R = 1}$).

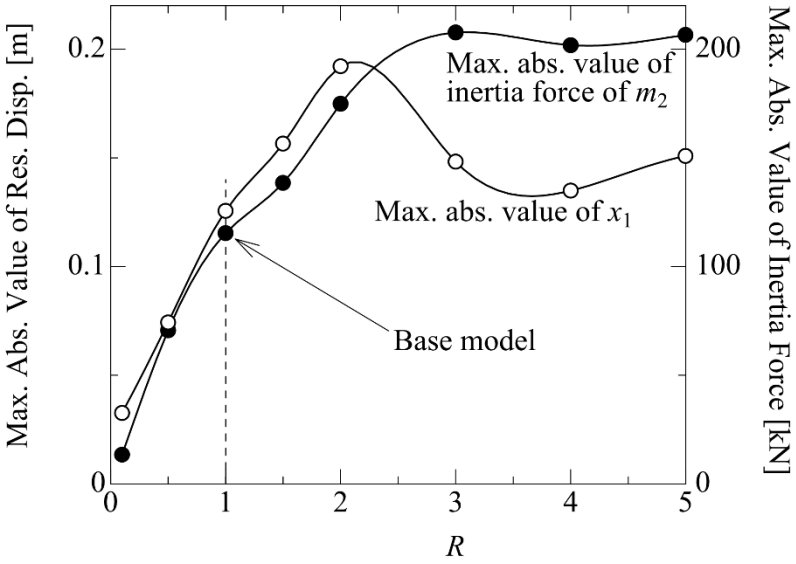

Figure 6. Maximum absolute values of x_1 and inertia force of m_2 as functions of scale factor R for m_2 ($S_1 = S_2 = 1$).

3.3. Cases where an Anti-Seismic Shelter is Installed and Connected to the Building via Damping Devices

In this subsection, the effects of installing a highly rigid anti-seismic shelter which can be regarded as a rigid body on the ground floor of the building and connecting that shelter to the first story ceiling beams via shock absorbers based on Kelvin-Voigt model is considered (Fig. 7). Although Matsumoto et al. [3] reported the results of analysis using the distinct element method (Nakagawa et al. [9]) for a similar model, if the objective is to determine the optimum specification of the viscous damper, the analysis applying the lumped mass model is far less time-consuming. The equation of motion for point mass m_1 has the form that the damping force term $C_a\dot{x}_1$ of viscous damper and the restoring force term $k_a x_1$ of elastic spring are added to the left side of Eq. (3).

$$m_1(\ddot{u} + \ddot{x}_1) + f_{D1} - f_{D2} + f_{R1} - f_{R2} + C_a\dot{x}_1 + k_a x_1 = 0 \qquad (10)$$

where C_a is the damping coefficient of the viscous damper, and k_a is the stiffness of the spring. The equation of motion for point mass m_2 is the same as in Eq. (4).

The relation between the damping coefficient C_a of the damper versus the maximum absolute value $|x_1|_{\max}$ of displacement of mass point~1 and the maximum absolute value $|m_2(\ddot{u} + \ddot{x}_2)|_{\max}$ of inertia force of mass point 2 (roof section) when the stiffness k_a of the spring is zero is shown in Fig. 8. As the value of C_a increases, $|x_1|_{\max}$ becomes smaller and asymptotically approaches zero. The maximum absolute value $|m_2(\ddot{u} + \ddot{x}_2)|_{\max}$ of the inertia force of m_2 is smaller than that of the fully rigid connection between the first story ceiling beams and the shelter when C_a exceeds about 10^5 N·s/m. After that, it reaches a local minimum around $C_a = 5 \times 10^5$ [N·s/m], and then gradually rises to a value close to that obtained when

the ceiling beams and the shelter are fully rigidly connected. Hence, for the present model, a damping coefficient C_a of about 5×10^5 N·s/m for the viscous damper connecting the building and the shelter can be deemed appropriate. The results of this analysis support the statement "In an existing two-story building without enough strength of the first story, the response of the first story can be significantly reduced by connecting a shelter, while the response of the second story increases. In this case also, the increase of the second layer response can be suppressed by connecting with oil dampers." as described in the Conclusions of the paper by Matsumoto et al. [3].

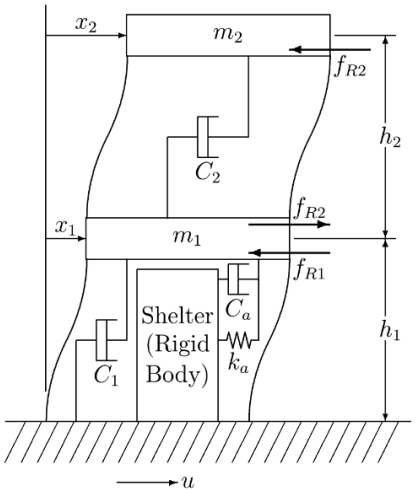

Figure 7. Two-story structure connected with shelter.

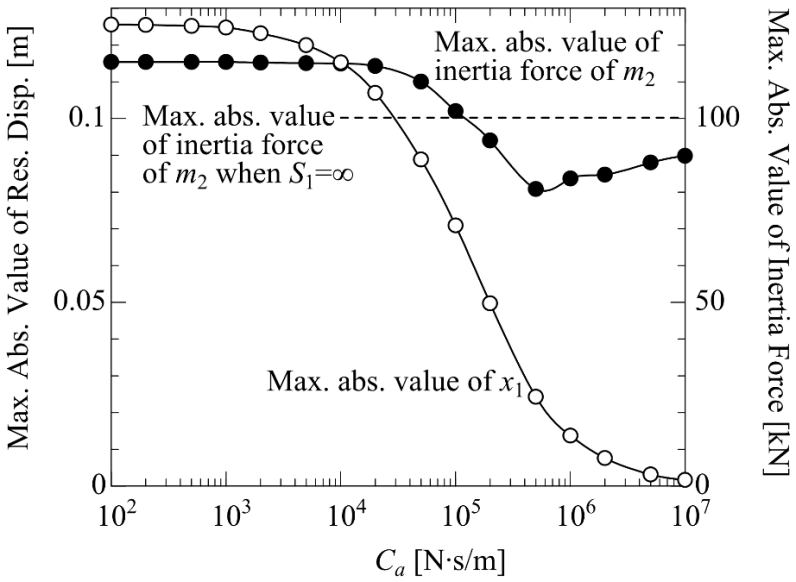

Figure 8. Maximum absolute values of x_1 and inertia force of m_2 as functions of damping coefficient C_a of dashpot ($S_1 = S_2 = 1$, $R = 1$, $k_a = 0$).

ISSN
2822-6895

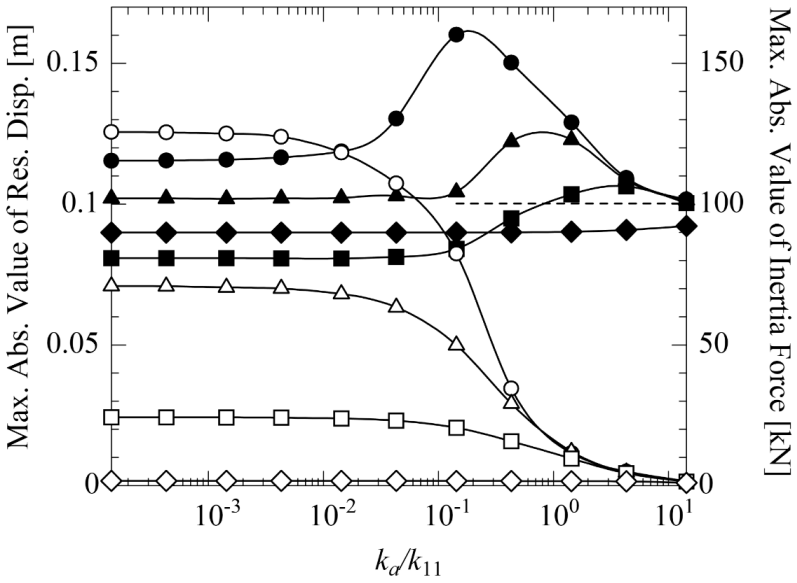

Figure 9. Maximum absolute values of x_1 and inertia force of m_2 as functions of spring constant k_a/k_{11} ($S_1 = S_2 = 1$, $R = 1$): open symbols, max. abs. values of x_1; closed symbols, max. abs. values of inertia force of m_2; circles, $C_a = 0$; triangles, $C_a = 10^5$ [N·s/m]; squares, $C_a = 5 \times 10^5$ [N·s/m]; diamonds, $C_a = 10^7$ [N·s/m]; dashed line, max. abs. value of inertia force of m_2 when $S_1 = \infty$.

Fig. 9 shows the relationship between the stiffness k_a/k_{11} of the spring versus the maximum absolute value $|x_1|_{max}$ of displacement of mass point 1 and the maximum absolute value $|m_2(\ddot{u} + \ddot{x}_2)|_{max}$ of inertia force of mass point 2 (roof section). In this graph, the maximum absolute value of the inertia force of m_2 rises rapidly from about $k_a/k_{11} = 10^{-2}$, so here also it can be said that the inertia force of the roof section may become excessive due to the increase of first story stiffness. The maximum absolute value of x_1 does not change significantly within the range of $k_a/k_{11} < 10^{-2}$, and there is little suppression of the deformation amount. It seems unnecessary to consider cases where k_a/k_{11} is larger than that, because the stiffness of springs used in shock absorbers is typically sufficiently small compared to story stiffness.

In order to determine the appropriate C_a, it is necessary to correctly identify the restoring force characteristics of the structure. However, since it is unrealistic to conduct full-scale experiments for each building, Araki et al. [1] proposed a method to predict the hysteresis model. Furthermore, the recent development of the Software for Collapsing Analysis of Wooden Houses “wallstat” has made it relatively easy to perform pushover (nonlinear static) analysis and to estimate the restoring force characteristics more accurately [6, 7].

4. CONCLUSIONS

In this study, the effect of first story stiffness on the inertia force of the roof section during an earthquake has been simulated, and guidelines for more effective seismic reinforcement have been considered. The following conclusions can be drawn from the above analysis:

1. Even if the stiffness of one part of a structure is increased, this may cause higher inertia forces in other parts of the structure during an earthquake. Hence, it is necessary to consider not only a part of the structure but also the whole structure in order to determine the seismic reinforcement method for multi-story buildings [multi-mass (multi-degree-of-freedom) structures].

2. When an anti-seismic shelter is installed on the ground floor of a building, the effect of seismic reinforcement is greater if the shelter is connected to the first story ceiling beams through appropriate damping devices than if the shelter is completely rigidly connected to the first story ceiling beams, because the absolute acceleration of the roof section during an earthquake can be suppressed more.

5. REFERENCES

[1] Araki, Y., Koshihara, M., Ohashi, Y. and Sakamoto, I., A Study on Hysteresis Model for Earthquake Response Analysis of Timber Structures, Journal of Structural and Construction Engineering (Transactions of AIJ) 579, (2004.5), 79-85 (in Japanese).

[2] Nakayama, S. and Kojima, K., Critical Earthquake Response of Wooden Houses Modeled by Single-Degree-of-Freedom Bilinear + Slip System Subjected to Pulse-Like Ground Motions, Journal of Structural and Construction Engineering (Transactions of AIJ) 780, (2021.2), 201-211 (in Japanese).

[3] Matsumoto, N., Matsumoto, K. and Ozawa, Y., Research on Response Control Method for Wooden Houses by Connecting Seismic Shelter, Journal of Structural Engineering 68B, Architectural Institute of Japan (2022.4), 442-451 (in Japanese).

[4] Newmark, N. M. and Rosenblueth, E., Fundamentals of Earthquake Engineering, (1971), 161-174, Prentice-Hall.

[5] Shibata, A., Newest Method of Design of Aseismic Structure, Rev. 3rd ed., (2021.9), 97-144, Morikita Shuppan (in Japanese).

[6] Nakagawa, T., Development of Analysis Method for Collapsing Behavior of Wooden Post-and-Beam Houses during Earthquake, Building Research Data 128, (2010) (in Japanese).

[7] Suzuki, T. and Nakagawa, T., Seismic Simulation wallstat Guide, (2020), Gakugei Shuppansha (in Japanese).

[8] Newmark, N. M. and Chan, S. P., A Comparison of Numerical Methods for Analyzing the Dynamic Response of Structures, Structural Research Series No. 36, Civil Engineering Studies, Engineering Experiment Station, College of Engineering, University of Illinois at Urbana-Champaign (1952.10).

[9] Nakagawa, T., Ohta, M., et al., Collapsing Process Simulations of Timber Structures under Dynamic Loading III: Numerical Simulations of the Real Size Wooden Houses, Journal of Wood Science 56, 4, (2010), 284-292.